

A Novel Tectal/Pretectal Population of Premotor Lens Accommodation Neurons

Paul J. May,¹⁻³ Paul D. Gamlin,⁴ and Susan Warren¹

¹Department of Neurobiology & Anatomical Sciences, University of Mississippi Medical Center, Jackson, Mississippi, United States

²Department of Ophthalmology, University of Mississippi Medical Center, Jackson, MS, United States

³Department of Neurology, University of Mississippi Medical Center, Jackson, Mississippi, United States

⁴Department of Ophthalmology and Visual Sciences, University of Alabama at Birmingham, Birmingham, Alabama, United States

Correspondence: Paul J. May, Department of Neurobiology & Anatomical Sciences, University of Mississippi Medical Center, 2500 North State Street, Jackson, MS 39216, USA; pmay@umc.edu.

Received: November 16, 2021

Accepted: January 3, 2022

Published: January 27, 2022

Citation: May PJ, Gamlin PD, Warren S. A novel tectal/pretectal population of premotor lens accommodation neurons. *Invest Ophthalmol Vis Sci.* 2022;63(1):35. <https://doi.org/10.1167/iovs.63.1.35>

PURPOSE. Under real-world conditions, saccades are often accompanied by changes in vergence angle and lens accommodation that compensate for changes in the distance between the current fixation point and the next target. As the superior colliculus directs saccades, we examined whether it contains premotor neurons that might control lens compensation for target distance.

METHODS. Rabies virus or recombinant rabies virus was injected into the ciliary bodies of *Macaca fascicularis* monkeys to label circuits controlling lens accommodation via retrograde transsynaptic transport. In addition, conventional anterograde tracers were used to confirm the rabies findings with respect to projections to preganglionic Edinger–Westphal motoneurons.

RESULTS. At time courses that rabies virus labeled lens-related premotor neurons in the supraoculomotor area and central mesencephalic reticular formation, labeled neurons were not found within the superior colliculus. They were, however, found bilaterally in the medial pretecal nucleus continuing caudally into the tectal longitudinal column, which lies on the midline, between the colliculi. A bilateral projection by this area to the preganglionic Edinger–Westphal nucleus was confirmed by anterograde tracing. Only at longer time courses were cells labeled in the superior colliculus.

CONCLUSIONS. The superior colliculus does not provide premotor input to preganglionic Edinger–Westphal nucleus motoneurons, but may provide input to lens-related premotor populations in the supraoculomotor area and central mesencephalic reticular formation. There is, however, a novel third population of lens-related premotor neurons in the tectal longitudinal column and rostrally adjacent medial pretecal nucleus. The specific function of this premotor population remains to be determined.

Keywords: oculomotor, superior colliculus, tectal longitudinal column, vergence, near triad

The superior colliculus or tectum allows animals to orient to or in some cases avoid the location of relevant sensory stimuli. To this end, it can help direct the eyes toward points of interest in animals with mobile globes, while at the same time helping to redirect attention. This critical capability of the superior colliculus to locate targets and direct the behavior of the animal with respect to them has been conserved across vertebrate lineages.¹ One property of target location is target distance. In the region of binocular overlap, adjusting the vergence angle between the eyes allows for stereopsis. In addition, changing the shape of the lens allows the target to be brought into focus, producing a sharp image on the retina. In humans and other primates with foveae and frontally located eyes, the capacity for detailed stereoptic vision has been maximized through fine control of the near response, which includes adjusting vergence angle, lens accommodation, and pupillary diameter with respect to target distance. It is not clear whether the superior colliculus

plays a role in controlling the eyes for these depth-related aspects of target fixation.

Most experimental investigations of collicular function have not tested for target distance.^{2,3} Microstimulation of the rostral superior colliculus in cats does produce changes in lens accommodation, although they are relatively small.⁴ Microstimulation of this region in the cat colliculus also produces convergence, and inactivating this region interferes with vergence.⁵ In monkeys, some researchers have found little evidence for activity related to vergence in the superior colliculus during disjunctive saccades.⁶ However, others have shown that microstimulation of the monkey superior colliculus does affect the vergence component of ongoing disjunctive saccades, as well as pure vergence movements.⁷⁻⁹ Furthermore, microstimulation of the rostral superior colliculus in macaques can produce vergence movements, and some cells in this area fire in relation to vergence movements that are not part of disjunctive saccades.^{10,11}

Microstimulation in the superior colliculus of monkeys also produces pupillary dilation,¹² and pupil changes appear to be part of a coordinated response to saccade targets.¹³

The pathways whereby the superior colliculus might control aspects of vergence, lens accommodation, and pupillary diameter are not clear. A projection by the superior colliculus to the supraoculomotor area (SOA) has been reported in the cat.¹⁴ In monkeys, this projection was described as terminating in the visceral motor column of the Edinger–Westphal nucleus.¹⁵ We have recently reinvestigated the projection of the superior colliculus to the SOA in monkeys.¹⁶ We found evidence that tectal terminals may contact the near response premotor neurons that are located in the SOA.^{17–21} However, we also noted labeled terminals within the preganglionic Edinger–Westphal nucleus (EWpg),¹⁶ suggesting the possibility that the superior colliculus might contain premotor neurons that could directly affect lens accommodation and pupillary diameter. In the present study, we investigated whether such a lens-related premotor population is present in the superior colliculus by injecting rabies virus into the ciliary body of macaque monkeys and looking for retrograde transsynaptic labeling of collicular neurons.

METHODS

The experiments were performed in 14 adult and young adult *Macaca fascicularis* monkeys. While both male and female animals were used, no pattern of sex-specific results was observed. The surgeries were approved by the Institutional Animal Care and Use Committees of either the University of Pittsburgh or the University of Mississippi Medical Center, depending on where the procedures took place. The experiments involving rabies virus were conducted with the aid of personnel from the Center for Neuroanatomy with Neurotropic Viruses at the University of Pittsburgh Medical Center. All animal procedures were carried out in adherence with the Guide for Care and Use of Animals and the ARVO Statement for the Use of Animals in Ophthalmic and Vision Research. Before surgery, the animals were sedated with ketamine HCL (10–15 mg/kg, intramuscular [IM]) to allow them to be intubated. They were anesthetized during surgery by isoflurane (1%–3%). For ciliary body injections, ophthalmic proparacaine drops were placed on the cornea. For central injections, animals received carprofen (3 mg/kg, IM) as a preemptive analgesic. These animals also were given atropine sulfate (0.05 mg/kg, IM) to inhibit mucous secretion and dexamethasone (2.5 mg/kg, intravenous) to suppress edema. The wound edges of the incision made for the central injections were infused with sensorcaine after closing. All animals were given an analgesic, buprenorphine (0.01 mg/kg, IM) or buprenex (0.001 mg/kg, IM), postoperatively.

Rabies Cases

The experiments done to identify the location of neurons controlling lens accommodation using rabies virus have been described previously with respect to the SOA and the central mesencephalic reticular formation population (cMRF) premotor populations,^{21,22} and readers are directed to those publications for details of the procedures. We injected the N2c strain of rabies virus ($1\text{--}5 \times 10^9$ plaque-forming units [pfu]/mL) into the ciliary body of the left

eye of each animal ($n = 8$). The injections of the ciliary body were made by driving a 25-gauge needle mounted onto a 100- μ L Hamilton syringe about 1 mm deep through the sclera at the outer border of the iris. The injections were spread across at least 12 sites along the dorsal, lateral, and ventrolateral portion of the iris. A variety of survival times (58 hours, $n = 1$; 66 hours, $n = 2$; 72 hours, $n = 1$; 76 hours, $n = 2$; 84 hours, $n = 2$) were used in order to follow the virus as it infected first-order neurons in the ciliary ganglion, second-order neurons in the EWpg, third-order premotor neurons, and fourth-order neurons supplying those premotor populations. At the end of the survival period, animals were deeply anesthetized with Na pentobarbital (50 mg/kg, intraperitoneal) and perfused through the heart with 4% paraformaldehyde in 0.1 M, pH 7.2 phosphate buffer (PB), followed by this solution with 5% glycerol added. After perfusion, the brains were blocked in the frontal plane and stored at 4°C in 4% paraformaldehyde in 0.1 M, pH 7.2 phosphate buffer with 10% glycerol as a cryoprotectant.

The brains were frozen sectioned at 50 μ m and collected into a 0.1 M, pH 7.2 phosphate Trizma buffer solution containing 0.05% sodium azide (PTA). Each ordered series of sections was placed in PTA with 1.5% normal horse serum and 0.5% Triton X-100 and then incubated in the same PTA solution that contained 1:1000 mouse monoclonal antibody to rabies virus. This antibody, designated 31G10, was a gracious gift of Dr. Matthias Schnell of Thomas Jefferson University, Philadelphia, Pennsylvania. It has been characterized and shown to be highly specific and effective.^{23,24} After a 2-day incubation at 4°C, the primary antibody was tagged using an ABC kit (Vector Labs, Burlingame, CA, USA) and then visualized using diaminobenzidine (DAB). Sections were mounted onto gelatin-coated slides, in some cases counterstained with cresyl violet, dehydrated, cleared, and coverslipped. A minimum of two 1-in-10 section series were processed per animal.

Recombinant Rabies Cases

We found that the labeled premotor neurons were distributed bilaterally. To determine whether this was due to bilateral projections to the EWpg by individual neurons, as opposed to overlapping populations of ipsilaterally and contralaterally projecting cells, we used recombinant rabies viruses that produced different fluorescent tags. The ciliary bodies in both eyes were injected as described above in four monkeys. However, in these cases, one eye received 150 μ L of solution containing 1×10^9 pfu/mL of an N2c recombinant rabies virus that produces the red fluorescent protein, mCherry (N2c-mCherry), and the other eye received 150 μ L of solution containing 1×10^9 pfu/mL of an N2c recombinant rabies virus that produces green fluorescent protein (N2c-GFP). These recombinant viruses were developed and gifted by Drs. Matthias Schnell and Christoph Wirblich of Thomas Jefferson University. (Details of the injection and processing procedures are found in a previous publication.²⁵) In this case, the animals survived 72 hours ($n = 1$), 76 hours ($n = 1$), and 80 hours ($n = 2$) before being sacrificed as described above.

After frozen sectioning at 50 μ m, every fifth section was processed to reveal the two markers using goat polyclonal antibody to GFP (Abcam #5450; Abcam, Cambridge, UK) and rabbit polyclonal antibody to DsRed, which cross-reacts with mCherry (Clonetechn #632496; Clonetechn, Mountain View,

CA, USA). Specifically, a solution of 1:200 goat anti-GFP and 1000 rabbit anti-DsRed was used in a 2-day incubation at 4°C. These primary antibodies were tagged with fluorescent secondary antibodies: specifically, donkey anti-goat IgG conjugated to green fluorescing Alexa Fluor 488 (#705-545-147; Jackson ImmunoResearch, West Grove, PA, USA) and donkey anti-rabbit IgG conjugated to red fluorescing Alexa Fluor 594 (Jackson ImmunoResearch #711-585-152). These were diluted 1:300 and 1:500, respectively, for a 2-hour incubation at room temperature. After mounting and drying, the sections were coverslipped under nonfluorescing medium. Adjacent cresyl violet-stained sections were used to determine cytoarchitectonic boundaries. An additional series was processed as described above for the regular rabies virus.

Conventional Tracer Cases

The rabies experiments revealed a previously undescribed set of EWpg afferents found in the medial pretectal nucleus and the tectal longitudinal column, which is located on the midline, between the colliculi. To confirm this novel finding, we used conventional anterograde tracers to examine this projection. In two animals, the midbrain was approached by aspirating the cortex above it, revealing the surface of the superior colliculus, caudal pole of the pulvinar, and the pineal gland. The tracer was held in a 1.0- μ L Hamilton syringe that was angled in the sagittal plane 22° tip rostral. The tip of the needle was positioned where the medial edge of the superior colliculus met the lateral edge of the pineal and the caudal edge of the pulvinar and was advanced 1.0 mm below the surface. In one case, 0.1 μ L of 10% biotinylated dextran amine (BDA) was injected. In the other case, 0.05 μ L of 3%

wheat germ agglutinin-conjugated horseradish peroxidase (WGA-HRP) was injected. The aspiration defect was then filled with Gelfoam, and the incision was closed with vicryl suture. The BDA animal survived 16 days and the WGA-HRP animal survived 2 days. The animals were then sedated with ketamine HCl (10 mg/kg, IM) and deeply anesthetized with Na pentobarbital (50 mg/kg) before being perfused through the heart with a buffered saline rinse, followed by a fixative containing 1.25% glutaraldehyde and 1.0% paraformaldehyde in 0.1 M, pH 7.2 PB. The brains were then blocked in the frontal plane and stored at 4°C in 0.1 M, pH 7.2 PB, with 30% sucrose as a cryoprotectant. The brains were frozen and sectioned on a sliding microtome at 80 μ m. The sections from the BDA injection were reacted using avidin-HRP with a nickel-cobalt DAB chromagen, as previously described.²⁶ A 1-in-3 series was counterstained with cresyl violet, and another was counterstained for cytochrome oxidase.²⁷ The sections from the WGA-HRP injection were reacted using tetramethylbenzidine with ammonium molybdate as a chromagen in 0.1 M, pH 6.0 PB, as previously described.²⁸ These sections were counterstained with cresyl violet. All sections were dehydrated in a graded series of ethanols, cleared in toluene, and coverslipped.

To document the results, labeled elements were charted and cells were illustrated using a BH-2 Olympus microscope (Olympus, Center Valley, PA, USA) equipped with a drawing tube. Low-magnification drawings were made using a drawing tube attached to a Wild M8 stereoscope (Leica Microsystems, Buffalo Grove, IL, USA). Photomicrographs were made using a Nikon DS-Ri1 digital camera mounted on a Nikon Eclipse E-600 photomicroscope equipped for light and fluorescence microscopy and employing Nikon Elements software as an interface (Nikon Instruments, Inc., Melville, NY,

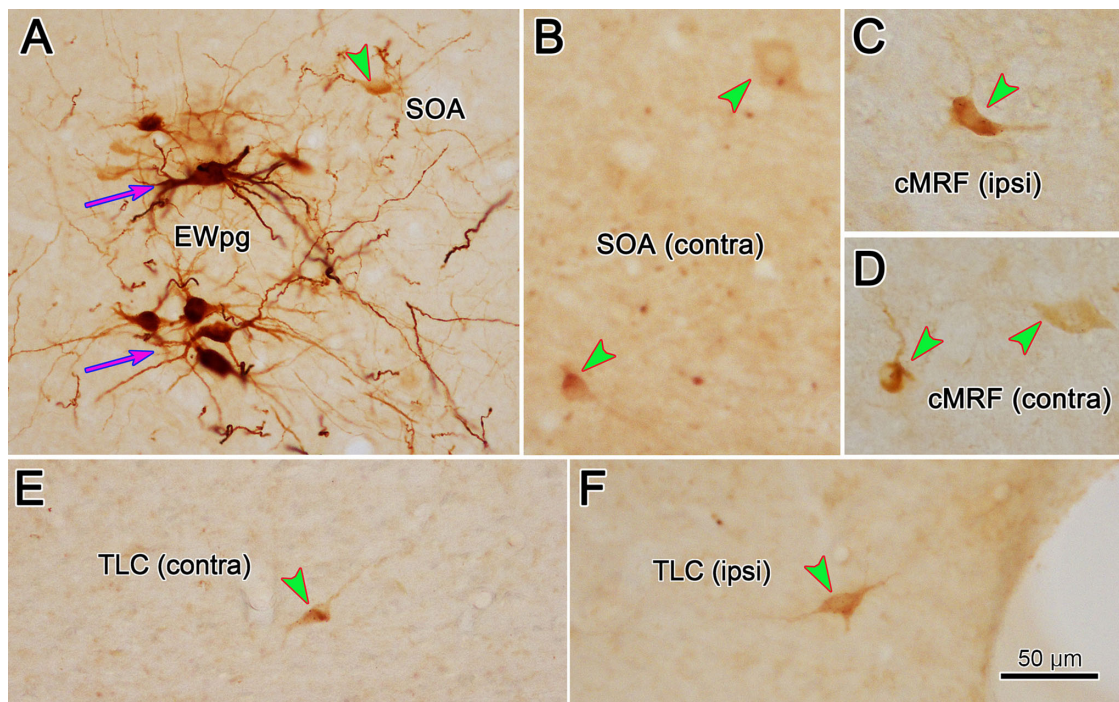


FIGURE 1. Labeling of motor and premotor populations 66 hours after injection of rabies virus into the left ciliary body. (A) Intensely labeled motoneurons (magenta arrows) were found in the left (ipsilateral) EWpg. Lightly labeled premotor neurons (green arrowheads) were found in the ipsilateral (left) SOA (A), contralateral (right) SOA (B), ipsilateral cMRF (C), and contralateral cMRF (D). Neurons with a similar light intensity were observed in the contralateral (E) and ipsilateral (F) TLC. Scale in F = A–E. Space on the right of F is a fiduciary mark.

USA). Image contrast and brightness were adjusted to match the viewed image using Adobe Photoshop (Adobe, San Jose, CA, USA).

RESULTS

Rabies Results

As shown previously,²¹ only motoneurons in the EWpg ipsilateral to the injection site were observed at the 58-hour survival time point (not illustrated). At 66 hours,

these EWpg motoneurons were heavily labeled (Fig. 1A, magenta arrows), and a few scattered, lightly labeled premotor neurons began to be observed in the SOA on both the side ipsilateral (Fig. 1A, green arrowheads) and contralateral (Fig. 1B, green arrowheads) to the injection site. Similarly, a few lightly labeled cMRF neurons were observed ipsilaterally (Fig. 1C) and contralaterally (Fig. 1D). We observed only one other population of labeled cells at this time point, which is shown in Figure 2. Outside of the heavily labeled motoneurons in the ipsilateral EWpg (red dots, Figs. 2A–D) and the lightly labeled premotor neurons (blue diamonds) found

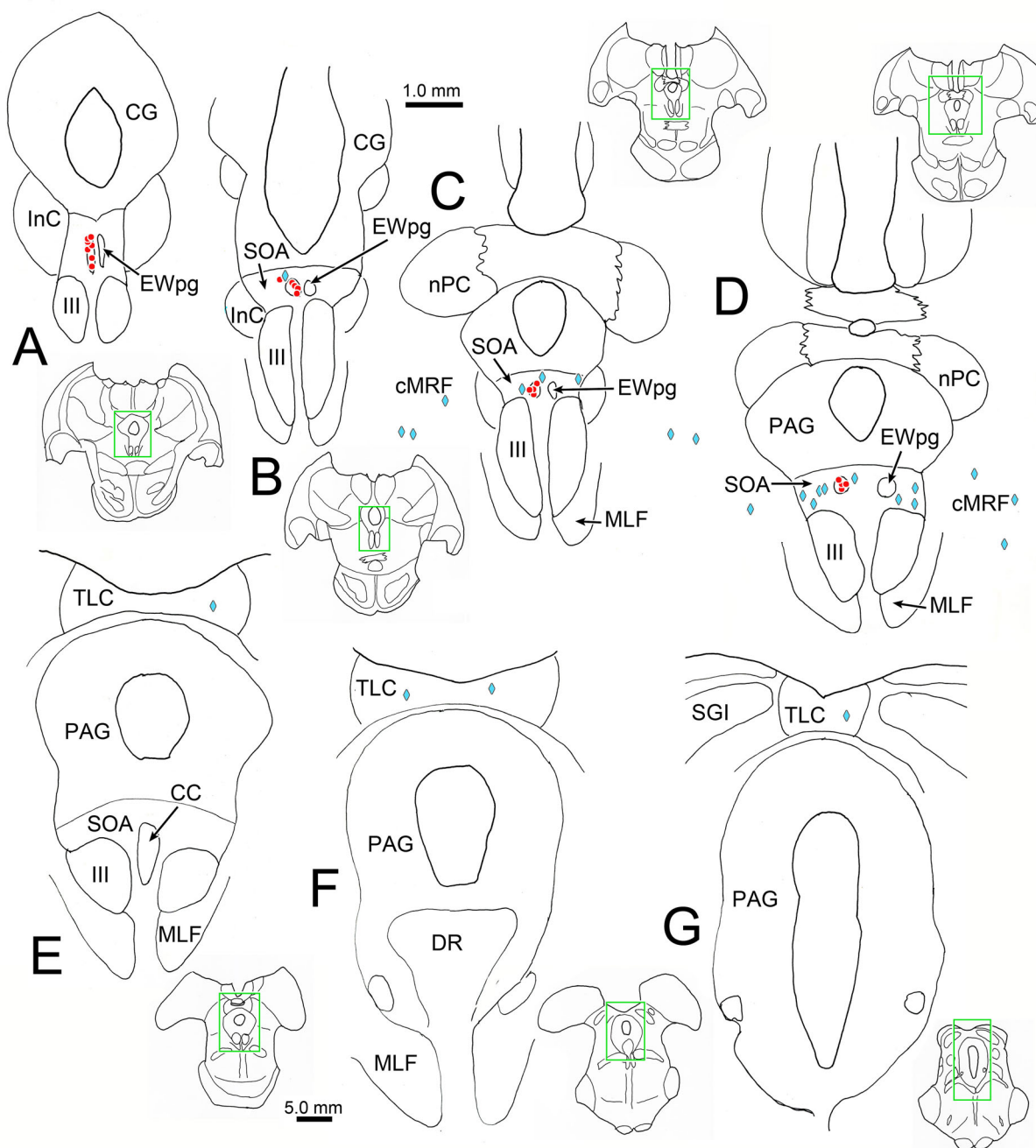


FIGURE 2. Distribution of labeled cells in the midbrain 66 hours after a left ciliary body injection of rabies. Intensely labeled neurons (red dots) were only observed in the EWpg ipsilateral to the ciliary body injection (A–D). A small number of lightly labeled cells (blue diamonds) were scattered bilaterally in the SOA (B–D) and the cMRF (C, D). In addition, a small number of lightly labeled cells were observed bilaterally in the TLC (E–G). Inserts of the entire section are provided to indicate the rostrocaudal level illustrated. Green boxes indicate region shown at higher magnification.

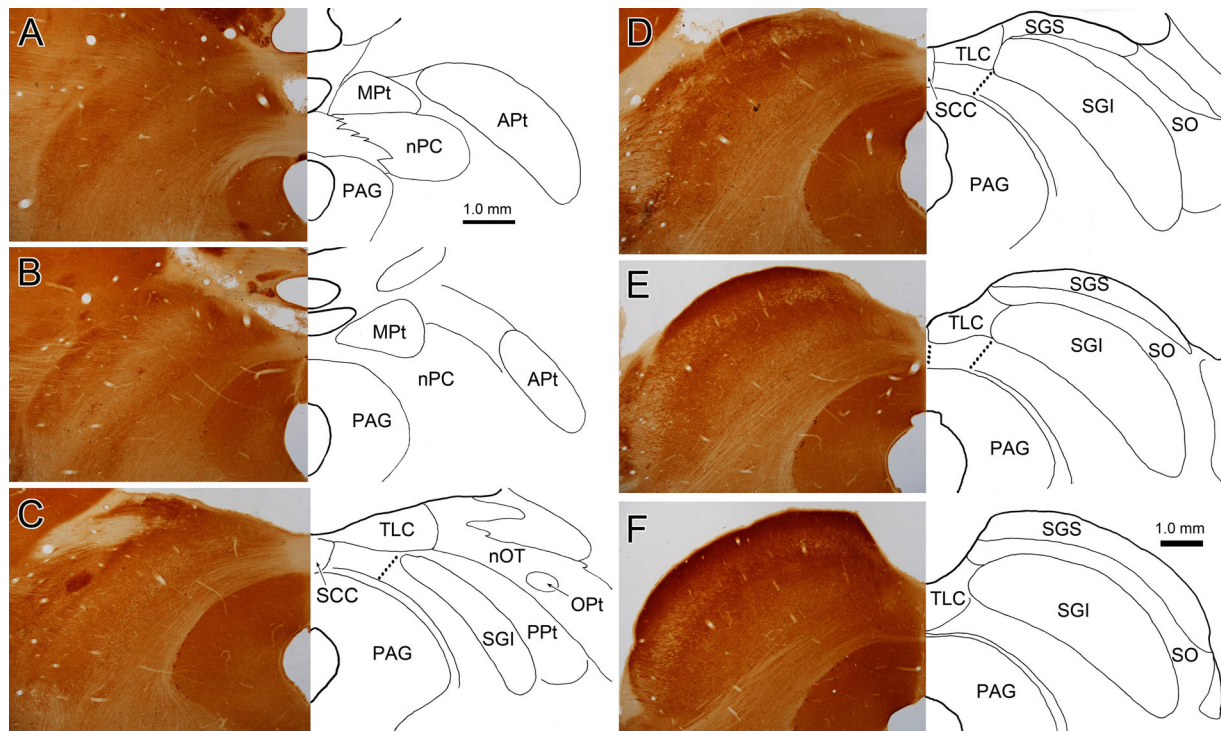


FIGURE 3. Cytochrome oxidase demonstration of the location of the MPT and TLC. The location of nuclear borders on the *right* is demonstrated with respect to cytochrome oxidase staining on the *left*. The MPT can be found lateral to the dorsomedial surface of the midbrain (A, B). This same region contains the TLC at more caudal levels (C–F). The possible borders of the ventral TLC are indicated by the *dotted lines*. We placed the caudal border of the MPT at the rostral border of the superior colliculus. Scale in F = A–E.

bilaterally in the SOA (Figs. 2B–D) and cMRF (Figs. 2C, 2D), a few lightly labeled cells were also present in the midbrain tectum in this case. These were located along the midline, between the colliculi (Figs. 2E–G), in the tectal longitudinal column (TLC). Like the SOA and cMRF premotor neurons, this scattered population was found on both sides of the brainstem. The degree of labeling in these tectal cells in the TLC is similar to that of the other premotor neurons (Figs. 1E, 1F) at this survival time.

The TLC was only recently described by Saldaña and colleagues.²⁹ They observed that the neuropil along the midline between the superior and inferior colliculi differs in terms of cytoarchitecture, neurochemical markers, and connectivity from either the adjoining superior colliculus or inferior colliculus, proper. They subdivided the rodent TLC into a ventral column, which displays auditory responses and is heavily interconnected with brainstem auditory centers,^{29,30,31} and a dorsal column that projects heavily to the lateral posterior and lateral dorsal nuclei of the thalamus.³² As this region has not been described in detail in the monkey, we examined it in cytochrome oxidase-stained sections (Figs. 3D–F). Note that the superficial gray layer of the superior colliculus (SGS) of the macaque does not extend all the way to the midline. The medial edge of the intermediate gray layer of the superior colliculus (SGI) is difficult to identify, but close examination suggests that it ends at approximately the same point as the SGS. This medial border is easiest to see in the cytochrome oxidase-stained sections with respect to the rostrocaudally oriented fibers in lower SGI.³³ (See May³⁴ for discussion of different collicular nomenclatures.) Alignment of the medial edge of the SGS and SGI is in agreement with physiologic reports that

describe the visual sensory maps of these two layers as being in register.^{35,36,37} In these cytochrome oxidase sections, the individual deeper layers, the intermediate white layer of the superior colliculus (SAI), and deep gray and white layers of the superior colliculus cannot be discriminated. The axons in these layers are seen to continue medially and cross the collicular commissure. However, based on previous findings in the monkey,²⁹ it is likely that this region represents the ventral part of the TLC, so we have indicated this with a dotted line in Figure 3. The SGI and TLC appear to extend further forward than the SGS due to the angle of the brainstem (Fig. 3C). The area containing the TLC then merges into the medial pretectal nucleus (MPT; Figs. 3A, 3B) without any clear border between them.

In the 72-hour survival case (not illustrated), the same areas displayed transsynaptically labeled cells: labeled motoneurons were found in EWpg, and labeled premotor neurons were found in SOA, cMRF, TLC, and the immediately adjacent MPT. However, the cells in these premotor regions were now well labeled. Labeled cells were not observed in the superior colliculus. At 76 hours, there were still well-labeled premotor neurons in these regions, and isolated, lightly labeled cells were apparent in other scattered locations, suggesting the virus had just begun infecting fourth-order neurons. Specifically, at 76 hours, well-labeled neurons (red dots) were found in the EWpg, SOA (Figs. 4A–D), and cMRF (Figs. 4A–D) within the midbrain tegmentum. An additional population of labeled neurons was observed near the midline in the midbrain tectum. Rostrally, they were located in the MPT (Figs. 4B, 4C), and the column of labeled cells then extended into the TLC (Figs. 4D–H). There were fewer labeled cells at caudal levels (Figs. 4G, 4H), and labeled cells

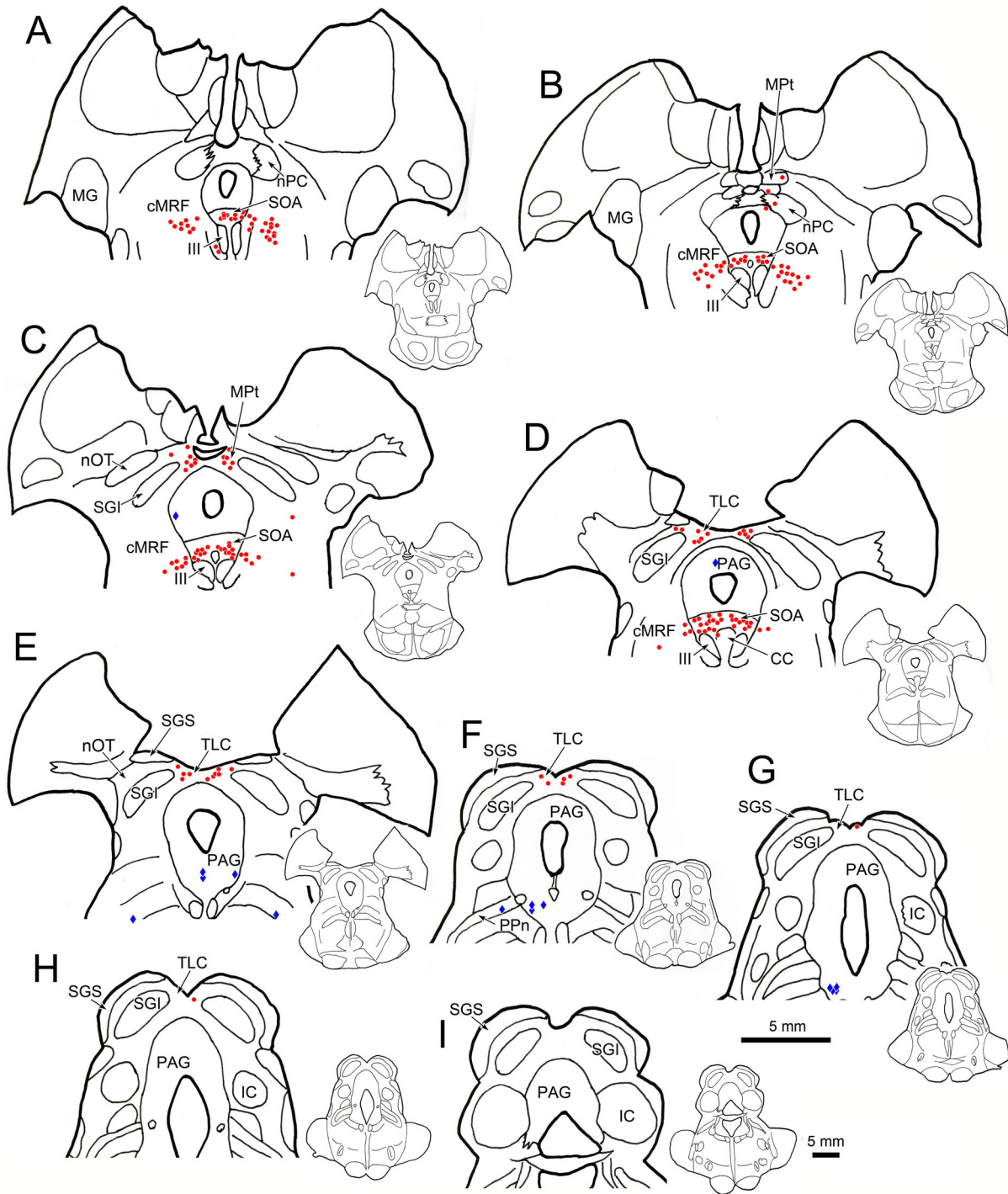


FIGURE 4. The distribution of neurons labeled by rabies virus 76 hours after an injection of the left ciliary body. Darkly labeled premotor neurons (red dots) are located bilaterally in the SOA (A–D) and in the cMRF (A–D). In addition, they are found dorsally in the MPt (B, C) and in the TLC (D–H). At this time point, scattered lightly labeled cells (blue diamonds) were present in other locations, including the periaqueductal gray (PAG) (C–G) and the peripeduncular nuclei (PPn) (E–G). Inserts of the entire section are provided to indicate the rostrocaudal level illustrated.

were not seen in the caudal end of the TLC (Fig. 4I). A few lightly labeled cells (diamonds) were observed in the periaqueductal gray (Figs. 4C–G) and the peripeduncular nucleus (Figs. 4E, 4F), but none were seen in the superior colliculus.

The tectal and pretectal cells had very distinctive morphology. In both the MPt (Fig. 5) and the TLC (Fig. 6), the labeled cells generally had relatively small, oval, or fusiform somata (short axis ~10 μ m). In most cases, only two or three primary dendrites extended abruptly from the soma.

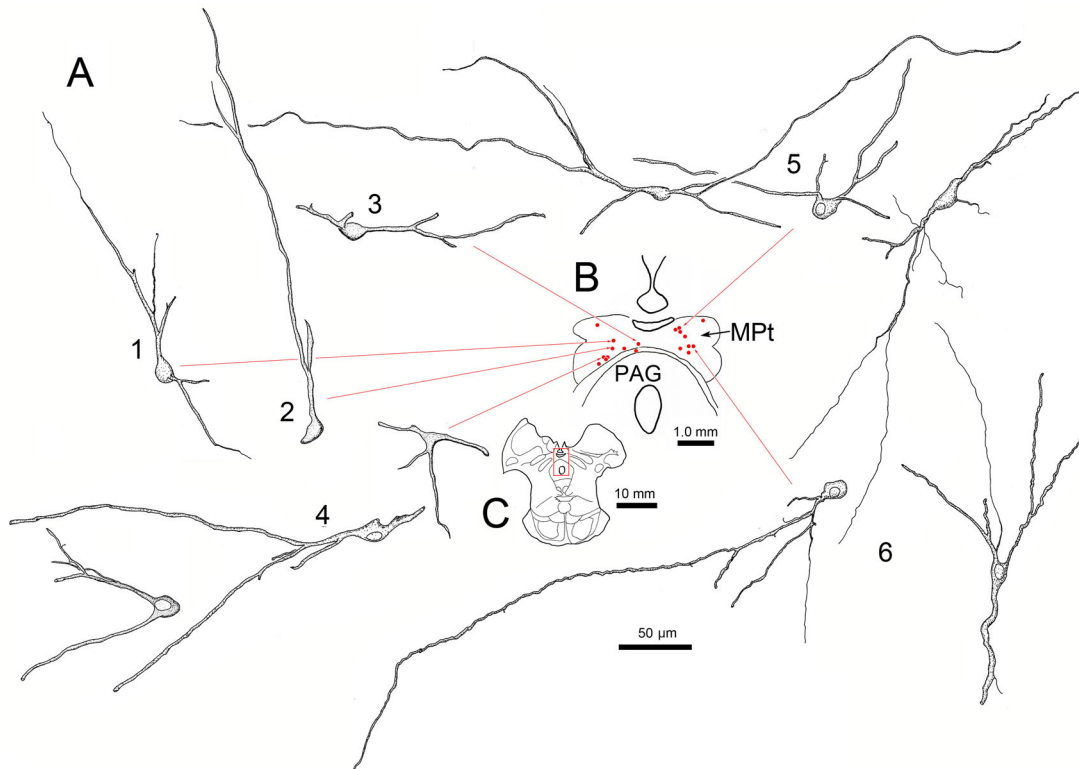


FIGURE 5. Morphology of lens premotor neurons in the MPT. Same case as shown in [Figure 4](#). Illustrations show examples of the somata and the dendritic arrangements of rabies-positive neurons (**A**₁₋₆) present in a single section (**B**, red dots) through the MPT. (**C**) Section containing labeled cells has red square to indicate sampled area in **B**.

Rarely were more than two branch points observed on these dendrites, even though they could be followed for up to 300 μm . The result of this pattern of arborization was a very simple dendritic tree that extended for long distances. Even though the EWpg was well labeled in these cases, relatively few cells were labeled in individual sections through the TLC and MPT. However, their long dendrites extended throughout the substance of the nuclei at the levels where somata were present. All these characteristics can also be appreciated in [Figure 7](#). Note the small ovoid labeled somata (thin yellow arrows), with long, poorly branched dendrites extending from labeled cells in both the MPT ([Figs. 7A, 7B](#)) and the TLC ([Figs. 7C-H](#)). There was no obvious pattern to the direction of dendritic field orientation. Some fields extended roughly parallel to the surface of the TLC, while others extended perpendicular to it. Most of the labeled cells were found dorsal to the commissural fibers crossing between the colliculi (red dots, [Figs. 6B, 6E](#)), but occasionally, a more ventral cell was present ([Fig. 6A](#)₅). In addition, it should be noted that the dendrites of labeled cells extended freely into the region containing the commissural fibers. Rostrally, at the level of the MPT, more cells were observed ventrally, adjacent to the periaqueductal gray ([Fig. 5A](#)₁₋₄).

Labeling of cells in the superior colliculus was not evident until we inspected the cases with an 84-hour survival time. At this later time point, we still observed labeled motoneurons in ipsilateral EWpg and labeled premotor neurons distributed bilaterally in the SOA and the cMRF (not illustrated). In the tectum, labeled neurons were present in the MPT ([Figs. 8A, 8B](#)) and in the TLC ([Figs. 8C-G](#)). An addi-

tional population was now present in the SGI of the superior colliculus ([Figs. 8C-G](#)). This labeled population was quite numerous and found throughout the rostrocaudal and dorsoventral aspects of the layer. Only the lateral aspect of the SGI lacked labeled neurons. In addition, a few cells were located in deeper layers of the colliculus ([Figs. 8C-F](#)), and an occasional cell was located in the optic layer, dorsal to the SGI ([Fig. 8G](#)). These labeled collicular neurons were also found on both sides of the midbrain (not illustrated). Other pre-premotor populations were also present at this time point in the midbrain, including in the posterior pretectal nucleus ([Figs. 8C, 8D](#)) and lateral to the MPT ([Fig. 8B](#)). Labeled neurons were present in a number of other locations at this survival time; for example, we have recently described the cells in the deep cerebellar nuclei labeled in these cases.³⁸

The labeling of the cells in the superior colliculus at this 84-hour time point varied among cells. Some were extensively labeled, revealing their dendritic morphology ([Figs. 9B, 9C](#), green arrows), while other cells were more lightly labeled, so that only punctate label in their soma and primary dendrites was observable ([Figs. 9B, 9C](#), magenta arrows). The lightly and densely labeled neurons were scattered randomly within the SGI ([Fig. 8](#), blue diamonds and red circles, respectively). The denser labeling allowed us to examine the morphology of the neurons. The cells were multipolar, with numerous primary dendrites extending out from them. The dendrites were relatively sparsely branched and extended for considerable distances within the layer. Most labeled cells were found in the SGI, but some could be seen in or below the SAI ([Figs. 9A, 9B](#)).

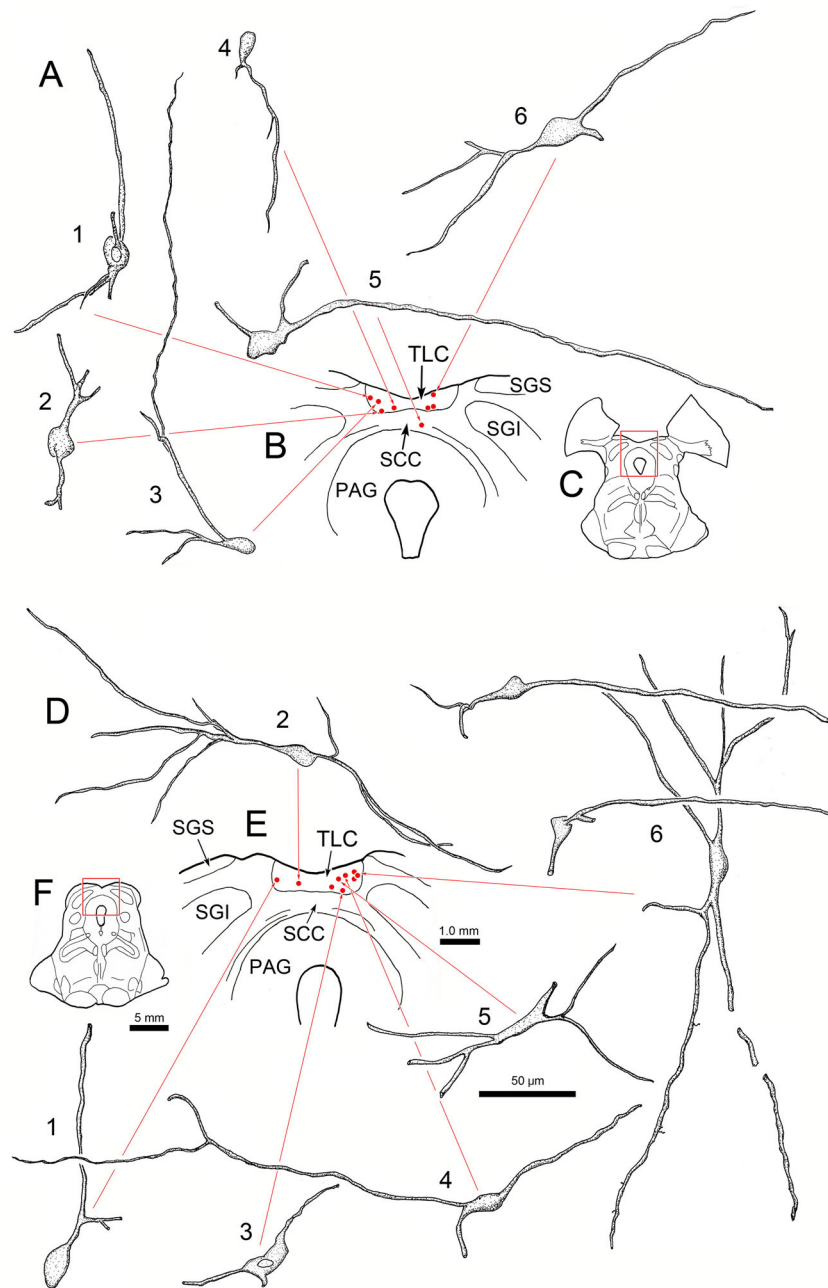


FIGURE 6. Morphology of lens premotor neurons in the TLC. Same case as shown in [Figure 4](#). Illustrations show examples of the somata and the dendritic arrangements of rabies-positive neurons (**A**₁₋₆ and **D**₁₋₆) present in individual rostral (**B**, *red dots*) and caudal (**E**, *red dots*) sections through the TLC. (**C**, **F**) Sections containing labeled cells have *red squares* to indicate sampled areas in **B** and **E**, respectively.

Conventional Tracer Results

The presence of lens premotor neurons supplying EWpg in MPT-TLC revealed here via transsynaptic transport of rabies virus is an entirely novel finding. These regions have received little investigation either physiologically or connectionally. We therefore examined this projection using conventional tracers. An injection of BDA that included portions of the TLC at the level of the rostral superior colliculus and spread into the medial edge of the SGI and deeper layers ([Figs. 10J, 10K](#)) produced considerable anterograde label dorsal to the oculomotor nucleus (III). Terminal arbors were labeled bilaterally in the SOA above the III

([Figs. 10B-I](#)), in the caudal central subdivision of the III ([Fig. 10I](#)), and in periaqueductal gray dorsal to the SOA ([Figs. 10B-I](#)), as previously described.¹⁶ Terminal fields were also found in the EWpg, on both sides of the midline ([Figs. 10C-H](#)). The density of the terminal labeling in EWpg was quite high. Examples of this can be seen in [Figure 11](#), where the sections were counterstained with cytochrome oxidase. This counterstain makes the motoneurons in both the III and the EWpg easy to recognize ([Fig. 11A](#)). Numerous BDA-labeled axonal arbors (arrows) were observed in both the ipsilateral ([Fig. 11B](#)) and contralateral ([Fig. 11C](#)) EWpg, adjacent to the cytochrome oxidase-positive, presumed preganglionic motoneurons (asterisks).³⁹

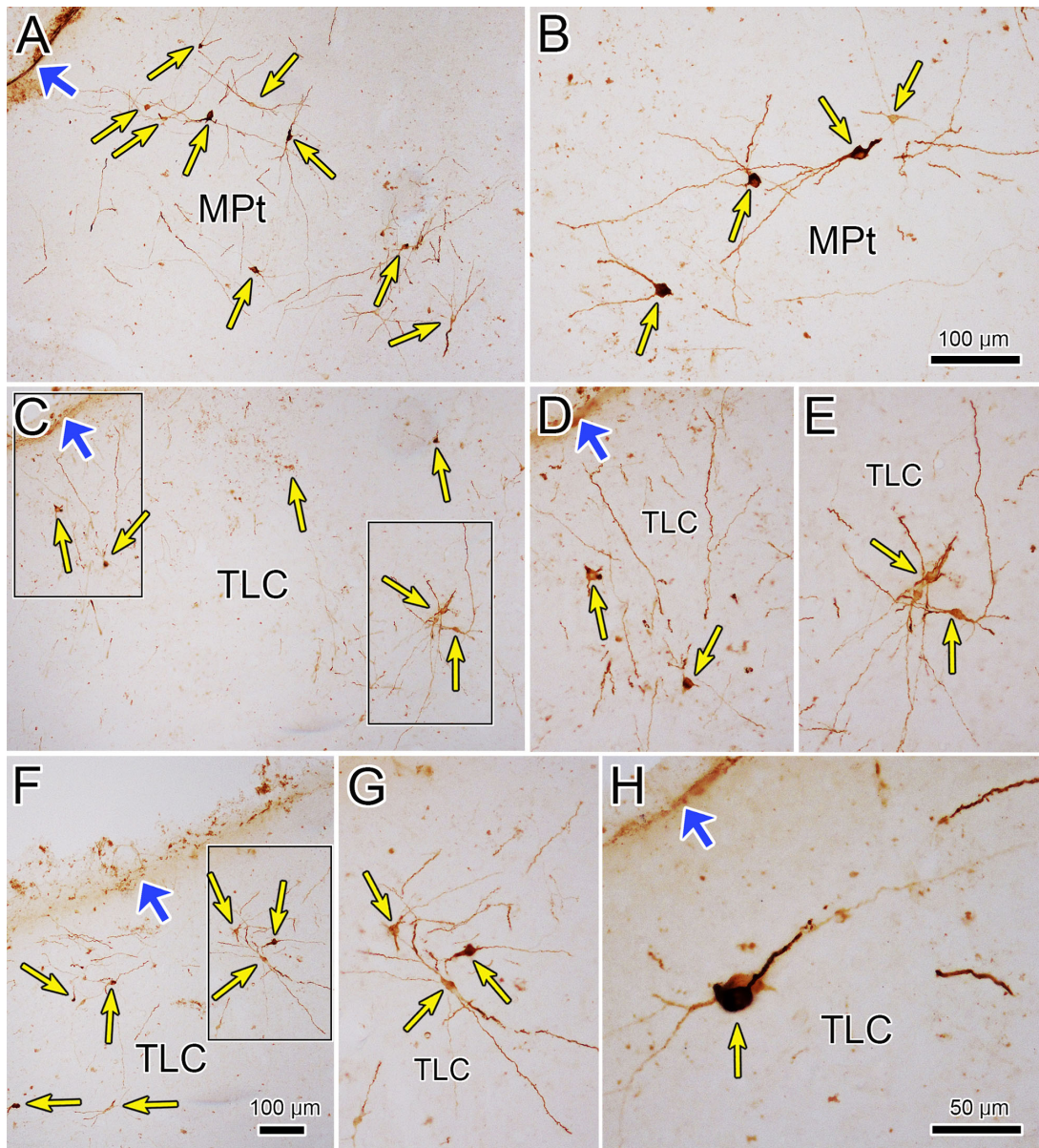


FIGURE 7. Dendritic organization of lens-related tectal premotor neurons. (A–H) Examples of neurons labeled by rabies virus 76 hours after the injection of the ciliary body are shown (*thin yellow arrows*). Note lack of dendritic branching and the wide extent of the dendrites. The relationship to the dorsal surface of the midbrain (*wide blue arrows*) is indicated. Boxes in C indicate examples shown at higher magnification in D and E. Box in F indicates example shown at higher magnification in G. Scale in F = A and C; in B = D, E, and G.

An injection of WGA-HRP that included the MPt, as well as the TLC (Figs. 12D–F), but also spread further into the superior colliculus, also produced bilateral terminal label in the EWpg (not illustrated). Of particular interest, this injection retrogradely labeled (red dots) neurons at a number of sites: the nucleus of the posterior commissure (Figs. 12B, 12C), the cMRF (Figs. 12C–E), the peripeduncular nuclei (Figs. 12D–G), and the periaqueductal gray (Figs. 12A–H). These sites would also show retrograde labeling with an injection confined to the superior colliculus³⁴ and so may have been labeled due to tracer spread. What is more noteworthy was the number of labeled cells present in the SOA (Figs. 12C–E), examples of which are shown in Figure 13. Far fewer cells were labeled in the SOA with retrograde tracer injections confined to the superior collicu-

lus,³⁴ suggesting the SOA may provide an input specifically to the TLC. It is also of interest that this injection also labeled cells within the ipsilateral TLC located caudal to the injection site (Figs. 12G, 12H). In addition, labeled neurons were present in the region around the central nucleus of the inferior colliculus (Figs. 12F–I).

Recombinant Rabies Results

We have previously examined the cases in which N2c-mCherry recombinant rabies virus was injected into the ciliary body of one eye and N2C-GFP recombinant rabies virus was injected into the ciliary body of the other eye to determine the laterality of premotor projection cells in the cMRF and SOA.²⁵ Here we examined labeling of premotor

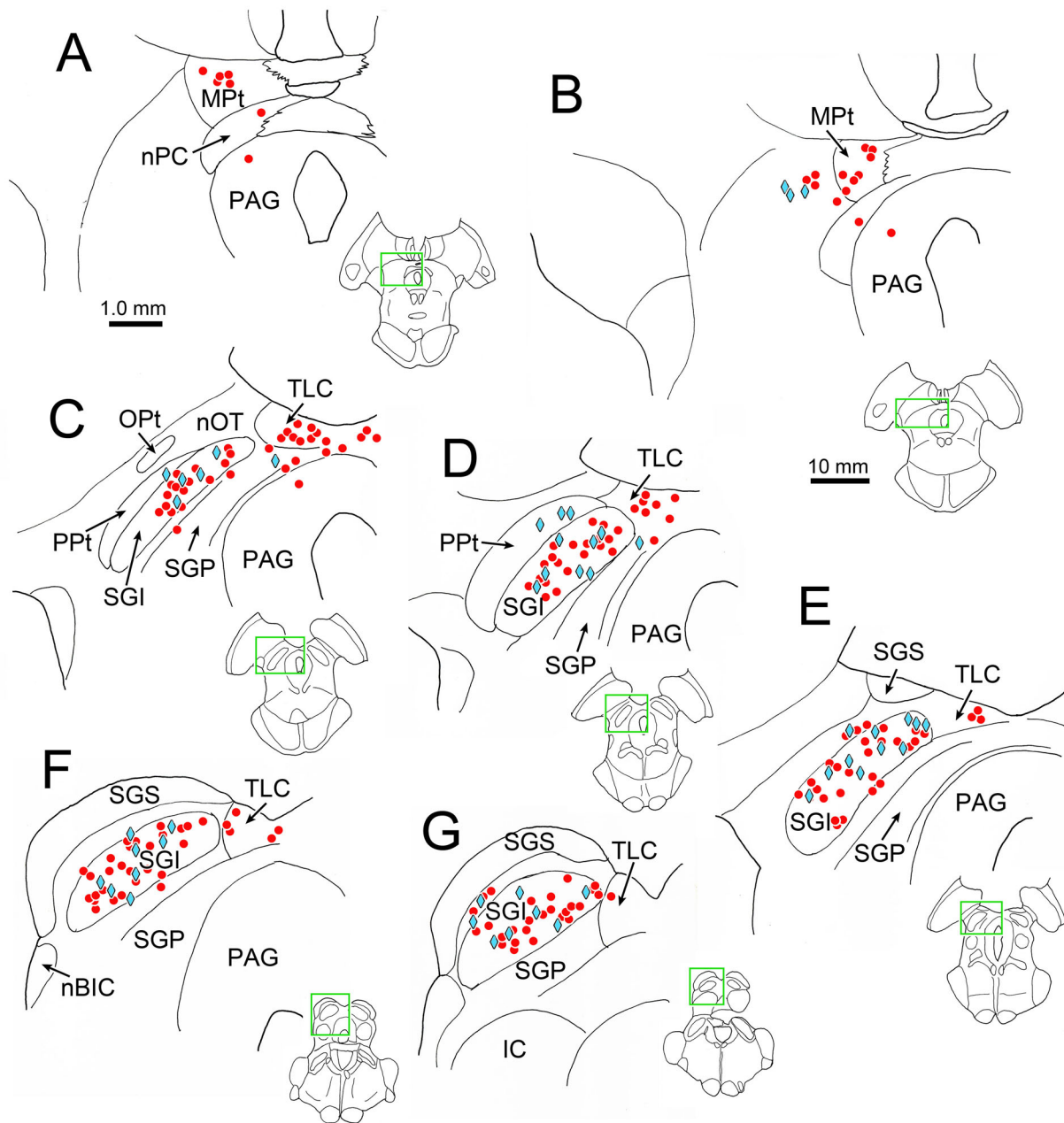


FIGURE 8. Distribution of rabies-labeled neurons in the midbrain 84 hours after an injection of rabies into the left ciliary body. Heavily labeled neurons (red dots) are present in the MPt (A, B) and TLC (C–G), as they were at earlier time points. However, an additional population of heavily labeled neurons was present in the superior colliculus (C–G), along with a more lightly labeled population (blue diamonds). The labeled cells are primarily located in the intermediate gray layer (SGI). Insets of the entire section are provided to indicate the rostrocaudal level illustrated. Green boxes indicate area sampled at higher magnification.

neurons in the MPt-TLC of the same cases. Labeling with the recombinant rabies virus lagged the labeling with nonrecombinant rabies. In the 72-hour survival animal, labeled cells were only present in the EWpg (not illustrated). In the 76- and 80-hour survival animals, premotor populations were labeled, but relatively few fluorescent-labeled cells were observed in the MPt and TLC compared to the SOA and cMRF. However, examination of adjacent sections stained using the antibody to rabies indicated that far more labeled cells were present than appeared via fluorescence. This suggests that (1) using the production of fluorescent

protein to tag infected cells is not as sensitive immunolabeling systems at these survival times and/or (2) the tectal premotor neurons may provide an environment that is less conducive to recombinant virus protein production. Nevertheless, the experiments were able to answer the question they were directed at.

As shown in Figure 14, fluorescent-labeled premotor neurons were present in the TLC at both the 76-hour (Figs. 14A, 14B) and 80-hour (Figs. 14C, 14D) survival time points. Double-labeled neurons were present that showed both the green (B₁ and C₁, green arrows) and red (B₂ and

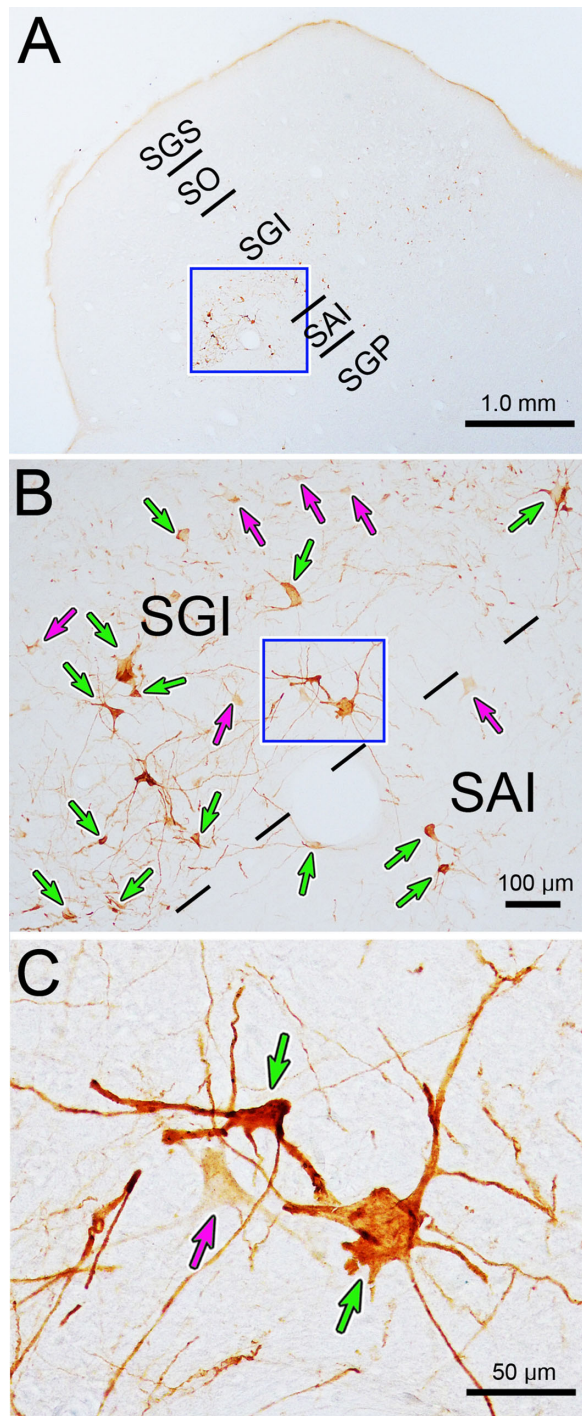


FIGURE 9. Somatodendritic morphology of neurons labeled in the intermediate gray layer (SGI) 84 hours after a rabies injection of the ciliary body. (A) Low-magnification view showing location of labeled neurons, primarily in the intermediate gray layer (SGI). Box indicates area sampled in B. Both densely labeled (green arrows) and lightly labeled (magenta arrows) neurons are present in the SGI and the intermediate white layer (SAI), as shown in B. Box indicates area sampled in C. The labeled neurons have multipolar somata, with numerous sparsely branched dendrites, as evident in C.

C₂, red arrows) fluorescent proteins were present, indicating these cells project bilaterally to the EWpg. This was further demonstrated by merging the images from the two filters (B₃ and C₃, yellow arrows), so that the double-labeled neurons took on a yellow or orange tinge. However, some single-labeled cells were also present. For example, Figure 14A shows a cell that did not fluoresce with the green filter (A₁) but fluoresced brightly with the red filter (A₂, red arrow). So this cell only projected to the ipsilateral EWpg, as confirmed by overlaying the images from the two filters (A₃, red arrow). Similarly, Figure 14D demonstrates adjacent cells, one of which fluoresced green (D₁, green arrow) and the other of which fluoresced red (D₂, red arrow). The close relationship of these two neurons is shown by the merged image (D₃, red and green arrows). In this case, the green cell projects contralaterally and the red one ipsilaterally.

DISCUSSION

Cells labeled by rabies virus were not present in the superior colliculus at survival times when immediate premotor neurons were labeled following injections of the ciliary body. This indicates that the superior colliculus does not directly control the motoneurons that modulate lens accommodation. However, multipolar cells found mostly in the SGI were labeled at longer survival times, suggesting the superior colliculus may supply the premotor neurons that in turn modulate lens accommodation. As these premotor populations also control the vergence and pupil size components of the near triad, these results suggest that indirect pathways are available that could allow the superior colliculus to modulate gaze behavior with regard to target distance. A previously undescribed population of tectal neurons is present in the TLC and the rostrally adjacent MPT that does supply direct input to lens-related motoneurons in the EWpg. The specific function of these cells, which make up a third premotor control center for lens accommodation, is currently unknown.

Technical Considerations

As previously detailed,²¹ examination of the superior cervical ganglion and spinal cord indicated that the rabies virus injected into the ciliary body had not involved the sympathetic pathways to the eye. Furthermore, at survival times when the premotor populations were labeled, the olivary pretectal nucleus was not. As this nucleus supplies the pupillary light reflex input to motoneurons in the EWpg,³⁴ this indicates the rabies virus did not infect terminals in the iris. The usual control series in which the primary or secondary antibodies are omitted were run, so the immunopositive tectal cells we observed are unlikely to be due to nonspecific labeling. We observed a few labeled cells outside of the three main premotor locations at 72- and 76-hour survival times. These may be minor contributors, or they may indicate that there is some overlap between the wave of labeling premotor populations and the initial labeling of afferents supplying the premotor populations. Overlap may occur because the time between injection and uptake of viral particles by individual postganglionic motoneuron terminals varies and/or because labeling times may be affected by axonal distances and terminal densities. However, the fact that the initial light labeling observed in MPT-TLC occurred at the same survival time as the initial labeling in the SOA and cMRF occurred

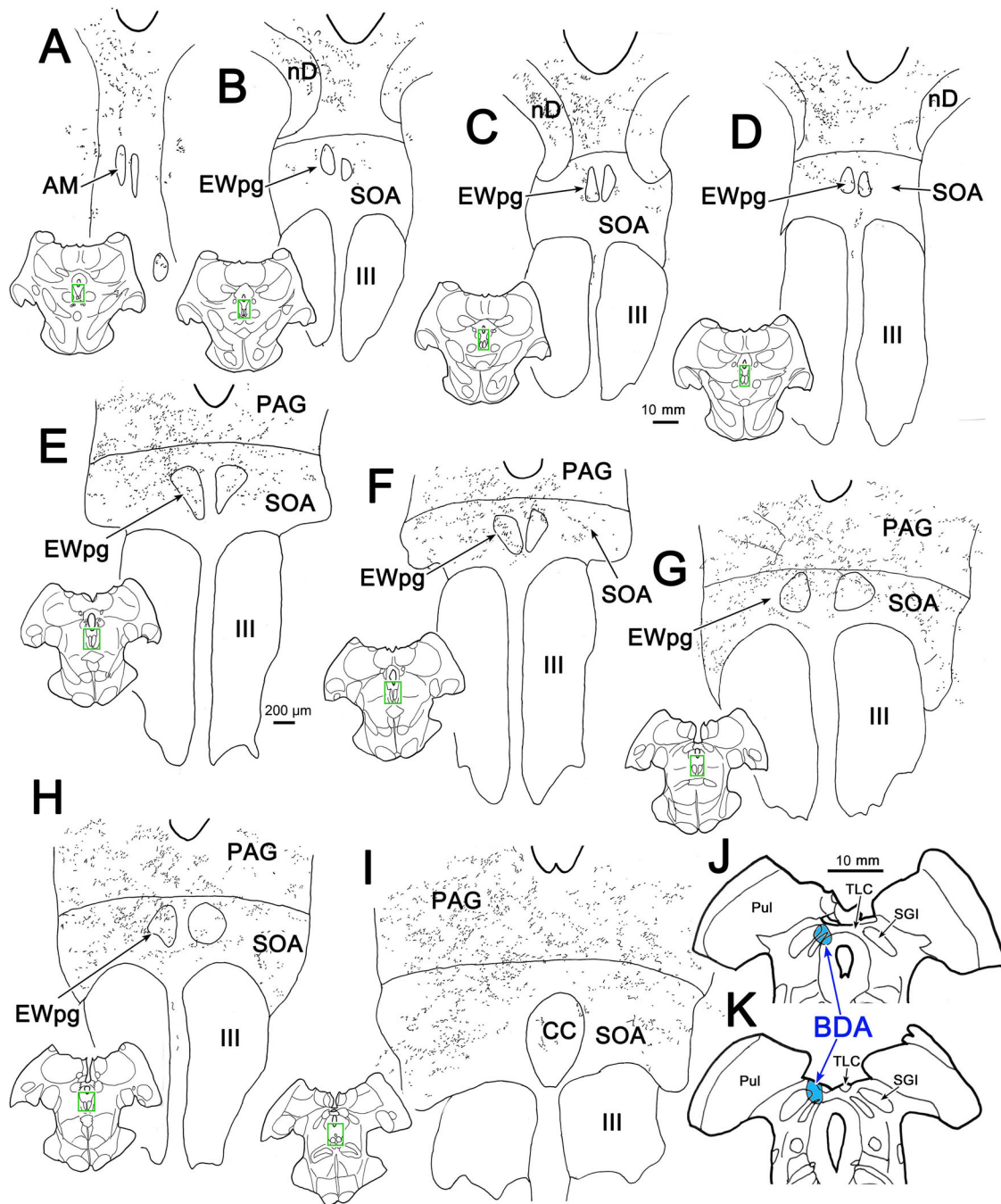


FIGURE 10. Projections of the TLC. A BDA injection of the TLC on the left also included the medial edge of the superior colliculus (J, K). This injection produced anterogradely labeled terminal arbors bilaterally, with an ipsilateral predominance, in the nucleus of Darkschewitsch (nD) (B–D), PAG (A–I), SOA (B–I), and the caudal central subdivision (CC) of the III (I). Labeled terminals were also present in the preganglionic EWpg on both sides (B–H). *Inserts* of the entire section are provided to indicate the rostrocaudal level illustrated. *Green boxes* indicate area sampled at higher magnification.

strongly suggests that this region also contains premotor neurons.

In the double-labeling experiments, the recombinant rabies virus did not label MPT and TLC cells as effectively as it labeled SOA and cMRF premotor neurons. For this reason, we did not attempt to quantify the results with respect to bilaterally and unilaterally projecting cells. However, the data did clearly support the contention that some of these

tectal cells project bilaterally to the EWpg. Care must be taken in assessing the unilateral populations. Since not all of the ciliary body was injected and not all of the preganglionic motoneurons were labeled, it is possible that some of singly labeled cells actually supply unlabeled EWpg motoneurons from the side that did not label the premotor cells.

We were not able to make injections of conventional tracers that were confined to the TLC. Tracer spread into the

superior colliculus makes interpreting the results of these injections more challenging. However, we feel that comparison between our cases with BDA injections confined to the superior colliculus¹⁶ and the one illustrated in **Figures 10** and **11** clearly indicates that the inclusion of the TLC in the injection considerably increases the terminal density in the EWpg, confirming the results from the rabies virus injections of the ciliary body.

Superior Colliculus Pathways

The data provided here support the contention that pathways are present that could allow the superior colliculus to modulate lens shape in order to compensate for target distance. The SGI may receive information on target distance from the visual association cortex. This has been specifically investigated in cats, where stimulation of the lateral supra-sylvian cortex produces lens accommodation, cells with lens-related activity can be antidromically driven from the superior colliculus, and there is anatomic evidence for projections to the SGI.^{40,41} In monkeys, cells that encode target depth information have been recorded in the lateral intraparietal cortex,⁴² and there is evidence that this information is provided to the superior colliculus.⁴³ The SGI may also receive vergence signals from the primate frontal eye field, as vergence-related activity has been reported there,⁴⁴ and it projects heavily onto the SGI.^{45,46,47} In light of these cortical inputs, the vergence-related activity reported in the superior colliculus,^{10,11} and the fact that vergence and lens accommodation are tightly coupled, it is perhaps not surprising that we observed neurons polysynaptically connected to the ciliary body within the SGI in the present study.

The presence of indirect, as opposed to monosynaptic, pathways connecting the superior colliculus to the EWpg parallels the pathways for collicular control over saccadic eye movement, which are also via inputs to premotor gaze populations.^{2,34,48} In the case of lens control, it is likely that this connection is via the premotor neurons located in the cMRF and/or SOA. In either case, it is unlikely that this pathway just controls lens accommodation in isolation and more likely that it also controls vergence angle.

With respect to the cMRF, this collicular projection probably targets premotor neurons that also control vergence changes during disjunctive saccades. The cMRF receives an extensive input from the superior colliculus via axon collaterals of predorsal bundle fibers destined for the gaze centers.^{26,49–53} These terminals target cMRF cells with descending projections to the brainstem and spinal cord.^{54–56} The cMRF is also known to project heavily and bilaterally onto the motoneurons in the EWpg.⁵⁷ The retrograde transsynaptic results presented here suggest that the cMRF neurons targeting preganglionic motoneurons also receive a direct projection from the superior colliculus. The cMRF also projects bilaterally onto medial rectus motoneurons, suggesting it plays a role in the vergence aspect of near triad function, as well.⁵⁸

There is relatively limited evidence for such a lens control pathway from physiologic experiments. However, microstimulation of the rostral portion of the cat superior colliculus does produce lens accommodation.⁴ The cMRF has primarily been associated with the production of horizontal conjugate saccades.^{50,59,60} However, more recently, evidence has emerged that it also plays a role in disjunctive saccades,⁶¹ based on microstimulation and the fact some cells in this region show eye-specific tuning. Furthermore,

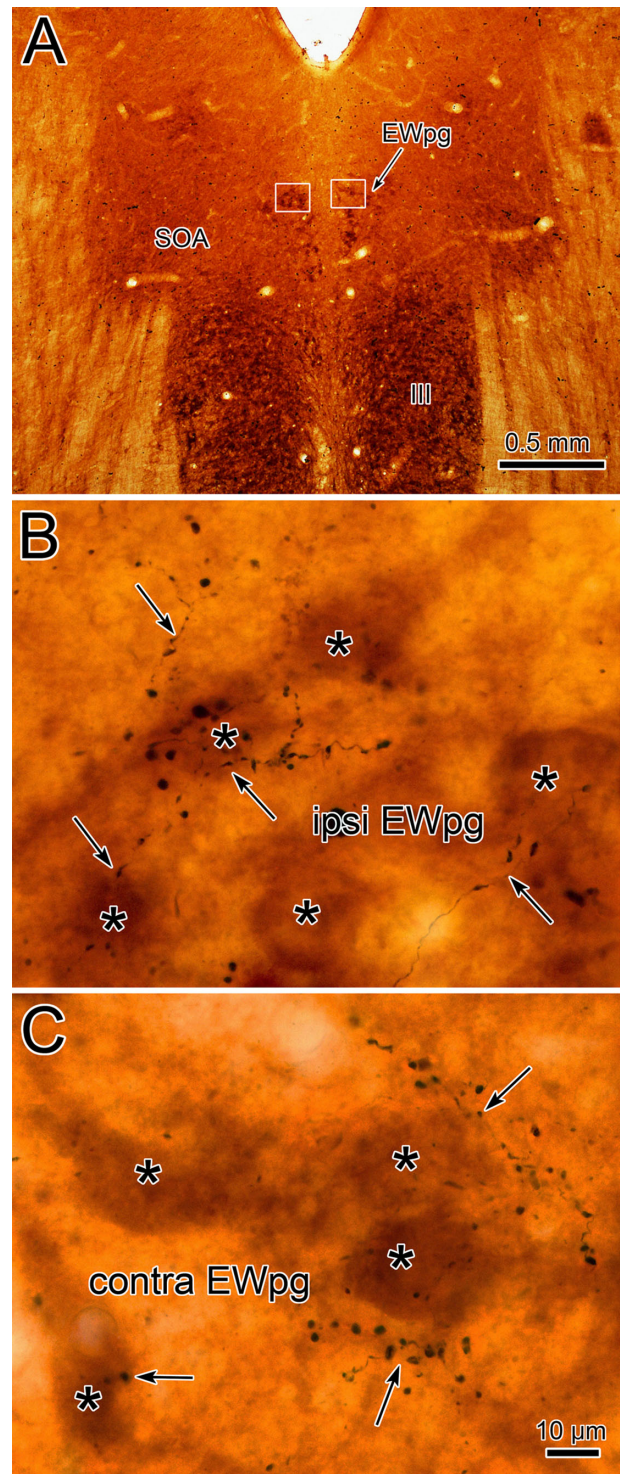


FIGURE 11. TLC terminals in the EWpg. (A) Cytochrome oxidase-stained sections reveal the location of the III and the EWpg. Boxes indicate the regions shown in **B** and **C**. Examples of the BDA-labeled axonal arbors (arrows) observed in the EWpg in the side ipsilateral (**B**) and contralateral (**C**) to the injection site (illustrated in **Fig. 10**). Large numbers of boutons are present in the vicinity of cytochrome oxidase-labeled presumed preganglionic motoneurons (asterisks). Scale in **B** = **C**.

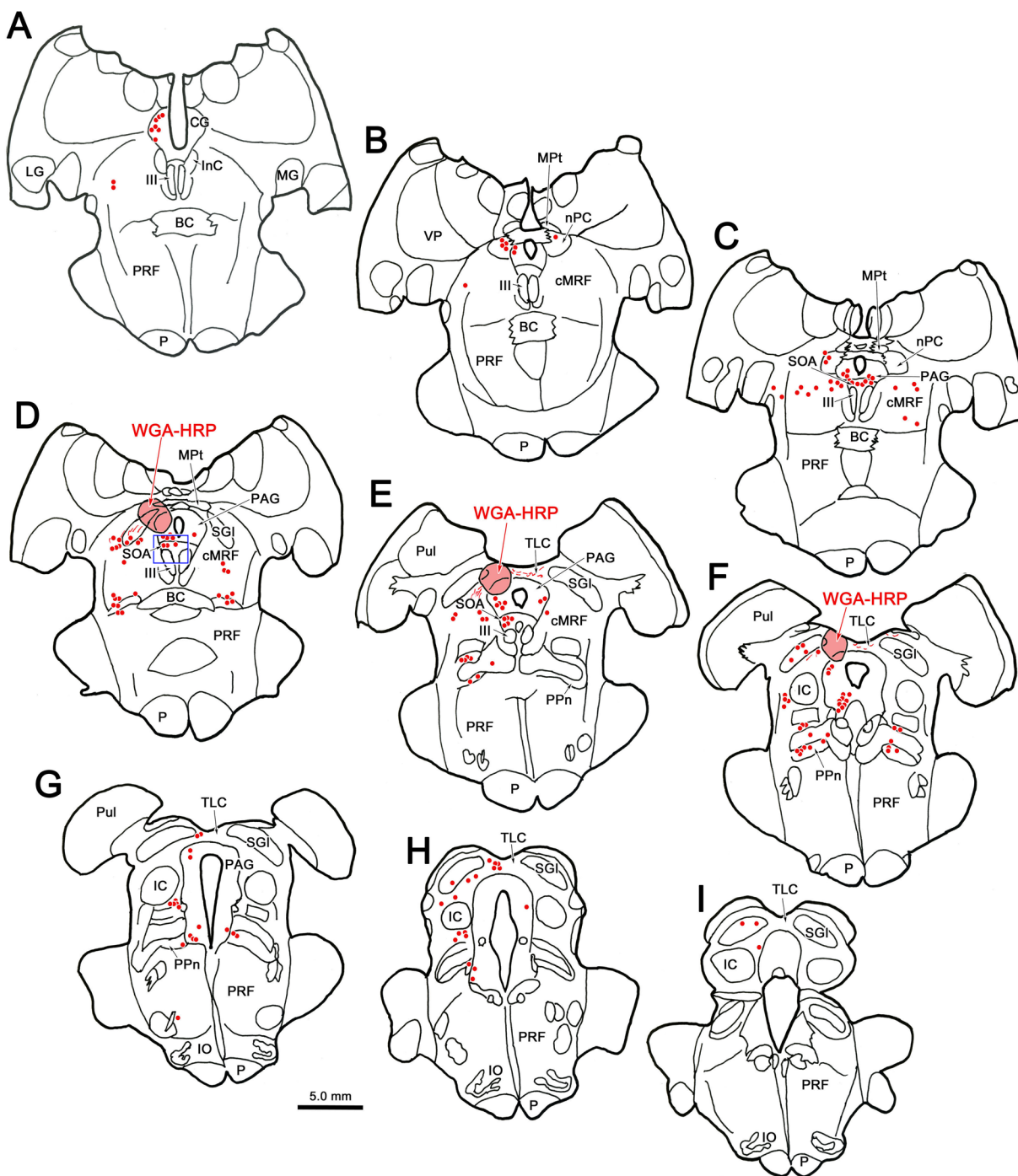


FIGURE 12. Possible MPT-TLC afferents. Many nuclei contained retrogradely labeled neurons (red dots) following an injection of WGA-HRP that included portions of the MPT (**D**) and the rostral part of the TLC (**E, F**) but that also spread into the medial superior colliculus (**D–F**). Among the structures containing labeled neurons were the central gray (CG) (**A**) and PAG (**B–H**), the nucleus of the posterior commissure (nPC) (**B, C**), cMRF (**C–E**), and peripeduncular nuclei (PPn) (**D–H**). Of particular note were the numerous labeled cells in the SOA (**C–E**) and in the TLC caudal to the injection site (**E–H**). *Boxed area in D is shown in Figure 13A.*

saccade-vergence burst neurons that fire with respect to vergence angle solely during disjunctive saccades have been recorded in the cMRF.⁶² It is certainly possible that cMRF cells firing for disjunctive saccades may also drive lens accommodation to compensate for target distance. Since collicular inactivation affects the vergence compo-

nent of disjunctive saccades,^{7,8} it is likely that a portion of the population of cells labeled by rabies virus in our longest survival animals may be supplying cMRF cells that project to the EWpg and/or to medial rectus motoneurons to produce compensation for target distance during disjunctive saccades. Of course, it is also possible that the

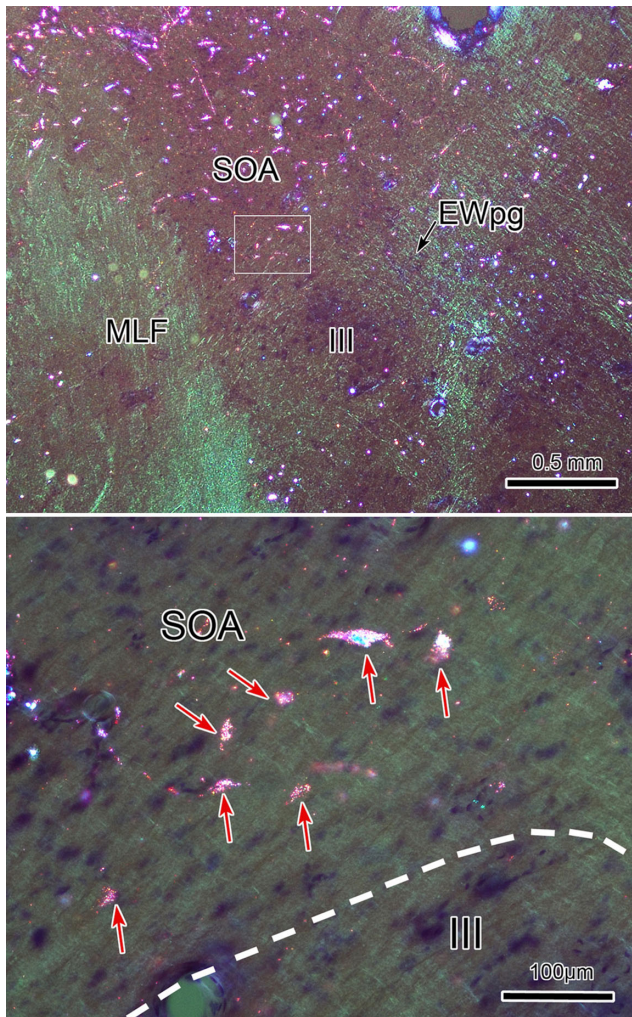


FIGURE 13. MPT-TLC afferent neurons in the SOA. Following the WGA-HRP injection shown in Figure 12, retrogradely labeled neurons (B, arrows) were numerous in the SOA. A shows the region containing SOA indicated by a box in Figure 12D. The boxed area in A is presented at a higher magnification in B. Retrograde tracer is revealed by crossed polarizer illumination.

collicular neurons labeled here fire for all types of saccades, and they were simply labeled because they happen to project upon cMRF neurons that fire for disjunctive saccades and project to EWpg. Unfortunately, transsynaptic transport of rabies virus simply reveals pathways, not function, per se.

It is possible that collicular inputs target premotor neurons that fire during symmetric vergence but do not fire during saccades. The vergence burst neurons found in the medial portion of the cMRF have these characteristics,⁶³ as do near response neurons located in the SOA that fire tonically to encode vergence angle.^{17,18,19,64} Most of the near response cells in the SOA also encode lens accommodation,⁶⁵ but vergence burst cells in the medial cMRF have not been tested in this regard. However, premotor neurons controlling lens accommodation have been demonstrated anatomically in both these regions.²¹ So it is also possible that the rabies-positive cells observed in the SGI following ciliary body rabies injections were labeled due to projections onto neurons that are involved in controlling symmetric, relatively slow, vergence eye movements. In agreement

with this, we have observed collicular terminals in close association with neurons in caudal SOA, which were retrogradely labeled by injections that involved the medial longitudinal fasciculus.¹⁶ We believe these are likely to be divergence neurons projecting to the abducens nucleus, as a similar population is revealed following rabies virus injections of the lateral rectus muscle.⁶⁶ While an argument can be made that conventional collicular saccadic burst neurons might provide an appropriate input for neurons in these regions that fire during disjunctive saccades,^{20,62} this type of input would not seem appropriate for neurons that do not fire during saccades of any type. On the other hand, recent investigations have shown that some collicular neurons are active during slower vergence eye movements.¹⁰ Such cells would provide an appropriate drive to near response premotor neurons in the SOA. It should be noted, however, that vergence units in the colliculus were observed only within the central retinal representation $<5^\circ$. The cells labeled by rabies in the present study were found throughout the SGI.

Another effect of collicular microstimulation is pupillary dilation.^{12,67} In the present study, we did not involve pupillary control pathways per se. However, the premotor neurons that control vergence and lens accommodation are generally believed to also modulate the activity of the pupillary sphincter muscle, as part of the near triad. The near triad premotor neurons can both increase and decrease pupil size, but collicular microstimulation always seems to produce dilation. Thus, collicular input to near response circuitry seems unlikely to be the substrate for these consistent pupillary dilation effects. Instead, collicular modulation of sympathetic pathways to the eye, perhaps via the locus ceruleus, is a more likely explanation of the microstimulation effects⁶⁸ than pathways through the cMRF and SOA.

Tectal Premotor Neurons

In our experiments, a set of neurons located in the TLC and the rostrally adjacent MPT were labeled by the rabies virus at survival times that indicate these are premotor neurons supplying the EWpg. To the best of our knowledge, this is an entirely novel finding. The similar morphology and the continuous distribution of the cells labeled following a rabies virus injection into the ciliary body strongly suggest that these cells represent a single population that does not respect the border between the two structures. This region also appears to be interconnected. We observed cells labeled more caudally in the TLC from a WGA-HRP injection of MPT and rostral TLC (Fig. 12), and MPT cells are labeled from dorsal TLC injections in the rat.³² While a significant number of cells were labeled over the rostrocaudal extent of the MPT-TLC region, due to their longitudinal arrangement, relatively few cells are present in any individual frontal section. Nevertheless, the unlabeled, counterstained neurons in these areas far outnumbered those labeled by virus. This suggests that while the MPT-TLC contains premotor neurons that control lens accommodation, this lens-related function is not likely to be the main role of the region. What these roles might be remains to be determined by recording from the lens-related and other neurons present in this area in awake behaving animals.

The MPT of the hamster, cat, and monkey is reported to receive a sparse retinal projection,⁶⁹⁻⁷² and the monkey retinotectal projection appears to extend medially into the dorsal TLC.⁷³ So it is possible that retinal inputs might modulate lens control through these cells. Other studies in the

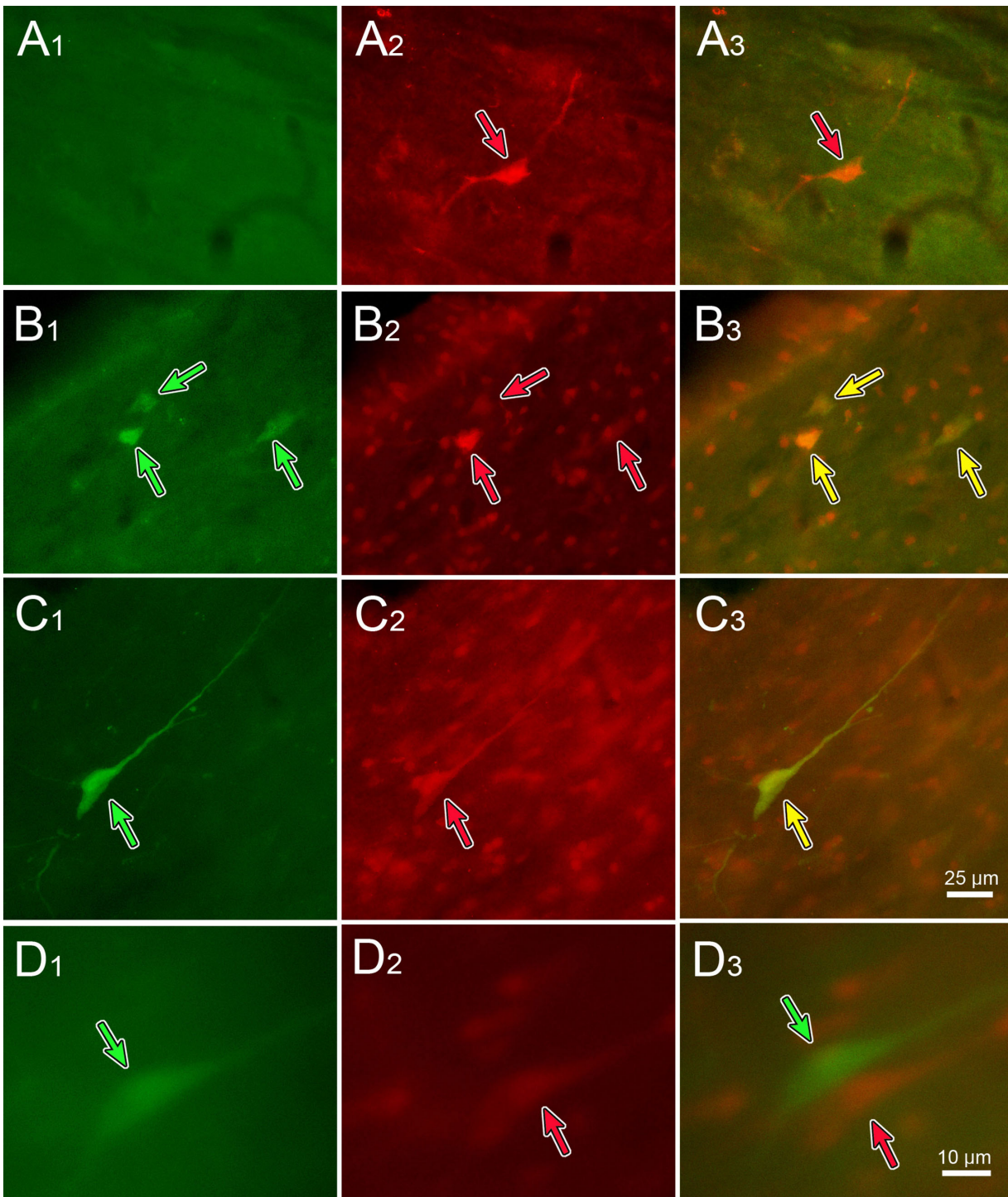


FIGURE 14. Some TLC neurons project to the Edinger–Westphal nuclei on both sides. Recombinant rabies virus injections were made into each ciliary body, with N2c-GFP injected on the left and Ns2c-mCherry injected on the right. Fluorescent images showing the GFP (*left column*), mCherry (*middle column*), and merged image (*right column*) are displayed. *Green arrows* indicate GFP-labeled neurons, and *red arrows* indicate mCherry-labeled neurons. Both singly labeled (**A**, **D**) and doubly labeled (*yellow arrows*) (**B**, **C**) were present. Scale in **C**₃ = **A**₁₋₃, **B**₁₋₃, **C**₁₋₂; in **D**₃ = **D**₁₋₂.

rat and cat have indicated that the MPT receives input from the intergeniculate leaflet and ventral lateral geniculate,^{74,75} nuclei that are believed to contribute to retinal modulation of circadian rhythms. Finally, there is recent evidence that the MPT in monkeys projects to the ventromedial hypothalamus, a region involved in defensive behaviors.⁷⁶ In cats, it

also projects to the central lateral nucleus of the thalamus,⁷⁷ as well as to the pulvinar/lateral posterior complex.^{78,79} The known thalamic targets of the dorsal TLC are the rat lateral posterior and lateral dorsal nuclei.³² As the pulvinar complex supplies parietal cortex with input, it seems possible that projections from the region supplying the EWpg with input

might also send a corollary discharge signal back to the lateral intraparietal cortex region that creates a target depth signal.

It is noteworthy that the TLC projection to the thalamus in rats appears to be GABAergic.³² If this is also true of the premotor neurons projecting to the EWpg, it would suggest that they are particularly involved in divergence, pupillary dilation, and lens accommodation for more distant targets. One of the unusual features of the near response neurons in the SOA is that most of the population fires for convergence and increased lens accommodation.^{17,18} Perhaps the MPT-TLC population represents the missing divergence component. The ventral TLC is reciprocally connected with the inferior colliculus^{29,31} and has cells that are responsive to auditory stimuli.³⁰ It seems unlikely that the lens premotor cells observed here would share inputs or functions with this population, although the dendrites of some premotor neurons extended into the ventral TLC.

One final point should be considered with respect to the location of this new population of lens-related premotor neurons. It seems highly likely that the axons of these cells access the EWpg via a route that takes them through the deep layers of the superior colliculus. Consequently, we must consider the possibility that previous studies that used electrical stimulation of the superior colliculus may have produced fiber-of-passage activation of these MPT-TLC axons. If these neurons control the far response, then we will have to reexamine whether changes in vergence or pupil size produced by collicular stimulation were actually produced by activating these MPT-TLC projections.

Acknowledgments

The support of the staff of the Systems Neuroscience Institute and the Center for Neuroanatomy and Neurotropic Diseases at the University of Pittsburgh Medical Center, as well as their director, Peter Strick, was instrumental in completing this study. In particular, the authors thank Isabelle Billig, who developed this recombinant rabies technique, for her extremely knowledgeable input. The authors also thank Christoph Wirblich and Matthias Schnell of Thomas Jefferson University for the gifts of recombinant rabies viruses and antibody to the rabies virus, as well as Ms. Jinrong Wei at the University of Mississippi Medical Center for technical assistance.

Supported by a grant from the National Institutes of Health EY014263 (PJM and PDG) and P30 EY03039 to University of Alabama at Birmingham.

Disclosure: **P.J. May**, None; **P.D. Gamlin**, AGTC (F), Editas Medicine (F), Lacerta Therapeutics (F), AAVANTIBio (F), Spotlight Therapeutics (F); **S. Warren**, None

References

1. Isa T, Marquez-Legorreta E, Grillner S, Scott EK. The tectum/superior colliculus as the vertebrate solution for spatial sensory integration and action. *Curr Biol*. 2021;31:R741–R762.
2. Sparks DL. The brainstem control of saccadic eye movements. *Nat Rev Neurosci*. 2002;3:952–964.
3. Gandhi NJ, Sparks DL. Changing views of the role of the superior colliculus in the control of gaze. In: Chalupa LM, Werner JS, eds. *The Visual Neurosciences*. MIT Press, Boston, MA, 2004:1449–1465.
4. Sawa M, Ohtsuka K. Lens accommodation evoked by microstimulation of the superior colliculus in the cat. *Vision Res*. 1994;34:975–981.
5. Suzuki S, Suzuki Y, Ohtsuka K. Convergence eye movements evoked by microstimulation of the rostral superior colliculus in the cat. *Neurosci Res*. 2004;49:39–45.
6. Walton MM, Mays LE. Discharge of saccade-related superior colliculus neurons during saccades accompanied by vergence. *J Neurophysiol*. 2003;90:1124–1139.
7. Chaturvedi V, van Gisbergen JA. Perturbation of combined saccade-vergence movements by microstimulation in monkey superior colliculus. *J Neurophysiol*. 1999;81:2279–2296.
8. Chaturvedi V, Van Gisbergen JA. Stimulation in the rostral pole of monkey superior colliculus: effects on vergence eye movements. *Exp Brain Res*. 2000;132:72–78.
9. Upadhyaya S, Meng H, Das VE. Electrical stimulation of superior colliculus affects strabismus angle in monkey models for strabismus. *J Neurophysiol*. 2017;117:1281–1292.
10. Van Horn MR, Waitzman DM, Cullen KE. Vergence neurons identified in the rostral superior colliculus code smooth eye movements in 3D space. *J Neurosci*. 2013;33:7274–7284.
11. Upadhyaya S, Das VE. Response properties of cells within the rostral superior colliculus of strabismic monkeys. *Invest Ophthalmol Vis Sci*. 2019;60:4292–4302.
12. Wang CA, Boehnke SE, White BJ, Munoz DP. Microstimulation of the monkey superior colliculus induces pupil dilation without evoking saccades. *J Neurosci*. 2012;32:3629–3636.
13. Wang CA, Munoz DP. Coordination of pupil and saccade responses by the superior colliculus. *J Cogn Neurosci*. 2021;5:1–14.
14. Edwards SB, Henkel CK. Superior colliculus connections with the extraocular motor nuclei in the cat. *J Comp Neurol*. 1978;179:451–467.
15. Harting JK, Huerta MF, Frankfurter AJ, Strominger NJ, Royce GJ. Ascending pathways from the monkey superior colliculus: an autoradiographic analysis. *J Comp Neurol*. 1980;192:853–882.
16. May PJ, Bohlen MO, Perkins E, Wang N, Warren S. Superior colliculus projections to target populations in the supraoculomotor area of the macaque monkey [published online November 11, 2021]. *Vis Neurosci*.
17. Mays LE. Neural control of vergence eye movements: convergence and divergence neurons in midbrain. *J Neurophysiol*. 1984;51:1091–1108.
18. Judge SJ, Cumming BG. Neurons in the monkey midbrain with activity related to vergence eye movement and accommodation. *J Neurophysiol*. 1986;55:915–930.
19. Das VE. Cells in the supraoculomotor area in monkeys with strabismus show activity related to the strabismus angle. *Ann N Y Acad Sci*. 2011;1233:85–90.
20. Pallus AC, Walton MM, Mustari MJ. Response of supraoculomotor area neurons during combined saccade-vergence movements. *J Neurophysiol*. 2018;119:585–596.
21. May PJ, Warren S, Gamlin PDR, Billig I. An anatomic characterization of the midbrain near response neurons in the macaque monkey. *Invest Ophthalmol Vis Sci*. 2018;59:1486–1502.
22. May PJ, Billig I, Gamlin PD, Quinet J. Central mesencephalic reticular formation control of the near response: lens accommodation circuits. *J Neurophysiol*. 2019;121:1692–1703.
23. Raux H, Iseni F, Lafay F, Blondel D. Mapping of monoclonal antibody epitopes of the rabies virus P protein. *J Gen Virol*. 1997;78:119–124.
24. Ruigrok TJ, van Touw S, Coulon P. Caveats in transneuronal tracing with unmodified rabies virus: an evaluation of aberrant results using a nearly perfect tracing technique. *Front Neural Circuits*. 2016;10:46.

25. May PJ, Gamlin PD. Is primate lens accommodation unilaterally or bilaterally controlled? *Invest Ophthalmol Vis Sci.* 2020;61:5.
26. Chen B, May PJ. The feedback circuit connecting the superior colliculus and central mesencephalic reticular formation: a direct morphological demonstration. *Exp Brain Res.* 2000;131:10–21.
27. Wong-Riley M. Changes in the visual system of monocularly sutured or enucleated cats demonstrable with cytochrome oxidase histochemistry. *Brain Res.* 1979;171:11–28.
28. May PJ, Warren S. Macaque monkey trigeminal blink reflex circuits targeting orbicularis oculi motoneurons. *J Comp Neurol.* 2021;529:2842–2864.
29. Saldaña E, Viñuela A, Marshall AF, Fitzpatrick DC, Aparicio M-A. The TLC: a novel auditory nucleus of the mammalian brain. *J Neurosci.* 2007;27:13108–13116.
30. Marshall AF, Pearson JM, Falk SE, Skaggs JD, Crocker WD, Saldaña E, Fitzpatrick DC. Auditory response properties of neurons in the tectal longitudinal column of the rat. *Hear Res.* 2008;244:35–44.
31. Aparicio M-A, Viñuela A, Saldaña E. Projections from the inferior colliculus to the tectal longitudinal column in the rat. *Neuroscience.* 2010;166:653–664.
32. Aparicio MA, Saldaña E. The dorsal tectal longitudinal column (TLCd): a second longitudinal column in the paramedian region of the midbrain tectum. *Brain Struct Funct.* 2014;219:607–630.
33. May PJ, Porter JD. The laminar distribution of macaque tectobulbar and tectospinal neurons. *Vis Neurosci.* 1992;8:257–276.
34. May PJ. The mammalian superior colliculus: laminar structure and connections. *Prog Brain Res.* 2006;151:321–378.
35. Goldberg ME, Wurtz RH. Activity of superior colliculus in behaving monkey: I. Visual receptive fields of single neurons. *J Neurophysiol.* 1972;35:542–559.
36. Wurtz RH, Goldberg ME. Activity of superior colliculus in behaving monkey: 3. Cells discharging before eye movements. *J Neurophysiol.* 1972;35:575–586.
37. Sparks DL, Hartwich-Young R. The deep layers of the superior colliculus. *Rev Oculomot Res.* 1989;3:213–255.
38. Bohlen MO, Gamlin PD, Warren S, May PJ. Cerebellar projections to the macaque midbrain tegmentum: possible near response connections. *Vis Neurosci.* 2021;38:E007.
39. May PJ, Sun W, Wright NF, Erichsen JT. Pupillary light reflex circuits in the macaque monkey: the preganglionic Edinger-Westphal nucleus. *Brain Struct Funct.* 2020;225:403–425.
40. Bando T, Yamamoto N, Tsukahara N. Cortical neurons related to lens accommodation in posterior lateral suprasylvian area in cats. *J Neurophysiol.* 1984;52:879–891.
41. Maekawa H, Ohtsuka K. Afferent and efferent connections of the cortical accommodation area in the cat. *Neurosci Res.* 1993;17:315–323.
42. Gnadt JW, Mays LE. Neurons in monkey parietal area LIP are tuned for eye-movement parameters in three-dimensional space. *J Neurophysiol.* 1995;73:280–297.
43. Gnadt JW, Beyer J. Eye movements in depth: what does the monkey's parietal cortex tell the superior colliculus? *Neuroreport.* 1998;9:233–238.
44. Gamlin PD, Yoon K. An area for vergence eye movement in primate frontal cortex. *Nature.* 2000;407:1003–1007.
45. Leichnetz GR, Spencer RF, Hardy SG, Astruc J. The prefrontal corticotectal projection in the monkey; an anterograde and retrograde horseradish peroxidase study. *Neuroscience.* 1981;6:1023–1041.
46. Huerta MF, Krubitzer LA, Kaas JH. Frontal eye field as defined by intracortical microstimulation in squirrel monkeys, owl monkeys, and macaque monkeys: I. Subcortical connections. *J Comp Neurol.* 1986;253:415–439.
47. Stanton GB, Goldberg ME, Bruce CJ. Frontal eye field efferents in the macaque monkey: II. Topography of terminal fields in midbrain and pons. *J Comp Neurol.* 1988;271:493–506.
48. Grantyn A, Brandi A-M, Dubayle D, Graf W, Ugolini G, Hadjidimitrakis K, Moschovakis A. Density gradients of trans-synaptically labeled collicular neurons after injections of rabies virus in the lateral rectus muscle of the rhesus monkey. *J Comp Neurol.* 2002;451:346–361.
49. Grantyn A, Grantyn R. Axonal patterns and sites of termination of cat superior colliculus neurons projecting in the tecto-bulbo-spinal tract. *Exp Brain Res.* 1982;46:243–256.
50. Cohen B, Waitzman DM, Büttner-Ennever JA, Matsuo V. Horizontal saccades and the central mesencephalic reticular formation. *Prog Brain Res.* 1986;64:243–256.
51. Moschovakis AK, Karabelas AB, Highstein SM. Structure-function relationships in the primate superior colliculus: I. Morphological classification of efferent neurons. *J Neurophysiol.* 1988;60:232–262.
52. Moschovakis AK, Karabelas AB, Highstein SM. Structure-function relationships in the primate superior colliculus: II. Morphological identity of presaccadic neurons. *J Neurophysiol.* 1988;60:263–302.
53. Zhou L, Warren S, May PJ. The feedback circuit connecting the central mesencephalic reticular formation and the superior colliculus in the macaque monkey: tectal connections. *Exp Brain Res.* 2008;189:485–496.
54. Perkins E, Warren S, May PJ. The mesencephalic reticular formation as a conduit for primate collicular gaze control: tectal inputs to neurons targeting the spinal cord and medulla. *Anat Rec.* 2009;292:1162–1181.
55. Wang N, Perkins E, Zhou L, Warren S, May PJ. Anatomical evidence that the superior colliculus controls saccades through central mesencephalic reticular formation gating of omnipause neuron activity. *J Neurosci.* 2013;33:16285–16296.
56. Wang N, Perkins E, Zhou L, Warren S, May PJ. Reticular formation connections underlying horizontal gaze: the central mesencephalic reticular formation (cMRF) as a conduit for the collicular saccade signal. *Front Neuroanat.* 2017;11:36.
57. May PJ, Warren S, Bohlen MO, Barnerssoi M, Horn AK. A central mesencephalic reticular formation projection to the Edinger-Westphal nuclei. *Brain Struct Funct.* 2016;221:4073–4089.
58. Bohlen MO, Warren S, May PJ. A central mesencephalic reticular formation projection to medial rectus motoneurons supplying singly and multiply innervated extraocular muscle fibers. *J Comp Neurol.* 2017;525:2000–2018.
59. Waitzman DM, Silakov VL, Cohen B. Central mesencephalic reticular formation (cMRF) neurons discharging before and during eye movements. *J Neurophysiol.* 1996;75:1546–1572.
60. Cromer JA, Waitzman DM. Neurons associated with saccade metrics in the monkey central mesencephalic reticular formation. *J Physiol.* 2006;570:507–523.
61. Waitzman DM, Van Horn MR, Cullen KE. Neuronal evidence for individual eye control in the primate cMRF. *Prog Brain Res.* 2008;171:143–150.
62. Quinet J, Schultz K, May PJ, Gamlin PD. Neural control of rapid binocular eye movements: saccade-vergence burst neurons. *Proc Natl Acad Sci USA.* 2020;117:29123–29132.
63. Mays LE, Porter JD, Gamlin PD, Tello CA. Neural control of vergence eye movements: neurons encoding vergence velocity. *J Neurophysiol.* 1986;56:1007–1021.

64. Das VE. Responses of cells in the midbrain near-response area in monkeys with strabismus. *Invest Ophthalmol Vis Sci.* 2012;53:3858–3864.
65. Zhang Y, Mays LE, Gamlin PD. Characteristics of near response cells projecting to the oculomotor nucleus. *J Neurophysiol.* 1992;67:944–960.
66. Ugolini G, Klam F, Doldan Dans M, Dubayle D, Brandi AM, Büttner-Ennever J, Graf W. Horizontal eye movement networks in primates as revealed by retrograde transneuronal transfer of rabies virus: differences in monosynaptic input to “slow” and “fast” abducens motoneurons. *J Comp Neurol.* 2006;498:762–785.
67. Wang CA, Blohm G, Huang J, Boehnke SE, Munoz DP. Multisensory integration in orienting behavior: pupil size, microsaccades, and saccades. *Biol Psychol.* 2017;129:36–44.
68. Szabadi E. Functional neuroanatomy of the central noradrenergic system. *J Psychopharmacol.* 2013;27:659–693.
69. Ling C, Schneider GE, Jhaveri S. Target-specific morphology of retinal axon arbors in the adult hamster. *Vis Neurosci.* 1998;15:559–579.
70. Hutchins B. Evidence for a direct retinal projection to the anterior pretectal nucleus in the cat. *Brain Res.* 1991;561:169–173.
71. Weber JT, Hutchins B. The demonstration of a retinal projection to the medial pretectal nucleus in the domestic cat and the squirrel monkey: an autoradiographic analysis. *Brain Res.* 1982;232:181–186.
72. Hutchins B, Weber JT. The pretectal complex of the monkey: a reinvestigation of the morphology and retinal terminations. *J Comp Neurol.* 1985;232:425–442.
73. Hubel DH, LeVay S, Wiesel TN. Mode of termination of retinotectal fibers in macaque monkey: an autoradiographic study. *Brain Res.* 1975;96:25–40.
74. Moore RY, Weis R, Moga MM. Efferent projections of the intergeniculate leaflet and the ventral lateral geniculate nucleus in the rat. *J Comp Neurol.* 2000;420:398–418.
75. Edwards SB, Rosenquist AC, Palmer LA. An autoradiographic study of ventral lateral geniculate projections in the cat. *Brain Res.* 1974;72:282–287.
76. Montardy Q, Kwan WC, Mundinano IC, Fox DM, Wang L, Gross CT, Bourne JA. Mapping the neural circuitry of predator fear in the nonhuman primate. *Brain Struct Funct.* 2021;226:195–205.
77. Graham J, Berman N. Origins of the pretectal and tectal projections to the central lateral nucleus in the cat. *Neurosci Lett.* 1981;26:209–214.
78. Kubota T, Morimoto M, Kanaseki T, Inomata H. Visual pretectal neurons projecting to the dorsal lateral geniculate nucleus and pulvinar nucleus in the cat. *Brain Res Bull.* 1988;20:573–579.
79. Schmidt M, Sudkamp S, Wahle P. Characterization of pretectal-nuclear-complex afferents to the pulvinar in the cat. *Exp Brain Res.* 2001;138:509–519.